

Theoretical Analyses of Aerosol Aging on a Substrate without Wall-Effects by a Cross-Flow

James P. Cowin^{1,†}, Xin Yang^{1,‡}, Xiao-Ying Yu^{*,2} and Martin J. Iedema³

¹Chemical and Materials Sciences Division, Pacific Northwest National Laboratory, Richland, WA 99354, USA

²Atmospheric Sciences and Global Climate Change Division, Pacific Northwest National Laboratory, Richland, WA 99354, USA

³Scientific Resources Division, W. R. Wiley Environmental Molecular Science Laboratory, Richland, WA 99354, USA

Abstract: Long time (~1day) aging or reactions of aerosol is typically studied using either large aerosol chambers (>10 m³) or particles supported on a substrate to minimize wall effects. To avoid wall effects in the latter, it is often essential that the wall reactivity be extremely small ($\ll 10^{-5}$ reactions per encounter) and that the particle loadings be very small (<1 pg/cm²) to eliminate transport-limited trace gas depletion near the particles and substrate. We evaluate here a cross-flow approach, which greatly reduces these constraints. Particles are to be supported on a micromesh (~50% or more open area) through which the reactive gas is drawn at around a few hundred cm/s. The analysis shows how the competitions between flow and diffusion establishes a “zone of isolation” several microns wide around each reactive particle, outside of which the reactivity of other particles or the substrate is irrelevant to the local reactions. This cross-flow approach reduces the effects of substrate and collective particle reactivity typically orders of magnitude, and will facilitate aging studies of supported aerosols.

Keywords: Aerosol aging, transport, diffusion, substrate, wall effect, cross-flow.

1. INTRODUCTION

Aerosols are an important component of the earth's atmosphere. They influence the climate by absorbing and scattering radiation or acting as cloud condensation nuclei and directly affect human health upon inhalation [1, 2]. Aerosols that are the most important to climate change and health have lifetimes on order of one to tens of days in the troposphere, and as long as several years in the stratosphere [3]. These times permit significant alteration of the physical and chemical properties of the aerosol particles. One of the most widely used ways to investigate the chemistry and aging of aerosols is *via* an aerosol chamber [4]. It allows the study of the interactions of gases with liquid and solid particles under conditions that mimic those of the atmosphere. However, increasingly large (> 10 m³) chambers are needed for studying aerosol aging for a day or more to limit wall effects such as particle loss. Many groups have used rigid or soft-walled large chambers such as bags. Such large chambers tend to suffer from one or more of the following disadvantages: expensive to build or expensive to operate, hard to find room for, limited ability to grossly

manipulate parameters like temperature or pressure, slow turn-around between experiments, and dangers of certain gross contaminations leading to very high expenses [4].

An alternative is to immobilize the aerosols on an inert substrate, for instance, on the inside wall of a flow tube [5]. But if the walls of the flow tube are too reactive, or the particles collectively are too reactive, the concentration of the reactive gases can be severely depleted near the walls, due to diffusive transport-limited flow. More than being just a nuisance, this transport-limited trace gas flow can easily invalidate this approach, whereby the rate of loss of trace gas becomes very insensitive to the particle reactivity, and the reaction extent (integrated rate on the particles) becomes either insensitive to the particle reactivity, or else becomes highly dependent upon insufficiently known quantities such as wall reactivity and local and global particle number density [3].

Flow cells usually have a density (ρ) of a reactive trace gas that might depend upon position along the length of the tube, but at any position along the length there would usually be a well defined value at the centerline, say of ρ_0 . Often one of the sought after reaction parameters is the particle's reactive uptake coefficient for that trace gas, γ_p , which is defined as the net probability of reaction per collision. If the walls, substrate, single particle, or particles collectively are too reactive, the trace gas density immediately adjacent to the aerosol particle surface (ρ_1) can be drastically reduced from the background density (ρ_0) value by the slow diffusion of the trace gas through the air. The situation is similar for particles deposited upon a substrate, across which a flow is drawn. Then ρ_0 is the asymptotic limit of the trace gas

*Address correspondence to this author at the Pacific Northwest National Laboratory, Atmospheric Sciences and Global Change Division, 902 Battelle Boulevard, P.O. Box 999, MSIN K9-30, Richland, WA 99354, USA; Tel: (509)3724524; Fax: (509)3726168; E-mail: xiaoying.yu@pnl.gov

†Temporary Address: Cowin In-Situ Science, LLC, Richland, WA 99354, USA

‡Temporary Address: Fudan University, Shanghai, People's Republic of China

density, far from the substrate. Detailed calculations are discussed in later sections.

The problem restated is that the derivative of ρ_1 with respect to γ_p , even normalized to γ_p , can approach zero and/or depend upon poorly known parameters, such as the wall or “substrate” uptake coefficient γ_s . The transport-limited trace gas reaction situation in coated wall flow systems is improved, if the total pressure is reduced. However, this problem is seldom eliminated for the usual-size flow tubes, unless the pressure is reduced until the trace gas mean free path λ becomes comparable to the tube diameter. This would typically require that there be no realistic levels of water vapor and oxygen (O_2). This is the approach used in a Knudsen cells [6, 7], with the total pressures ≈ 1 mbar and λ of about 3 cm. Even when the unrealistic water and O_2 levels are acceptable, it is very important, in a Knudsen cell (or flow tube), to have only a single or partial layer of particles. Otherwise severe trace gas depletion can occur as it diffuses into the underlying layers [8, 9].

We detail here how a cross-flow through a substrate can be very effective in removing these collective “wall effects”. The approach generally assumes that the particle reaction extent is going to be followed either in real-time or, after specific periods of exposure, using sufficiently sensitive tools such as infrared spectroscopy or ex-situ elemental analysis such as in a scanning electron microscope equipped with energy dispersed x-ray analysis [10]. The cross-flow, we show, should reduce the effects of substrate reactivity by at least 1000 times when compared to the multiple particle static reactor [10]. The cross-flow design is simple and versatile, and for studies of slow reactions and long time particle aging, could easily be the method of choice compared to large aerosol chambers.

2. METHOD: CROSS-FLOW TO REMOVE WALL EFFECTS

It is well-known that particles can be easily supported on a variety of strong and inert micromesh substrates. These are available from many manufacturers, for instance, electron microscope suppliers offer them as 3 mm discs, which are suited for transmission or scanning electron microscopy (TEM or SEM). These substrates can be obtained in different

materials such as carbon, silicon, silicon nitride, silicon oxide, diamond, and polymers. Fig. (1) shows some typical TEM substrates including “lacey carbon”, Quantifoil carbon, and nuclepore-type membranes. Supported particles are seen on the lacey carbon and Quantifoil carbon micromesh membranes. These substrates usually have 10 to 100 nm thickness, an active diameter of about 2 to 2.5 mm, submicron webbings, and 50% to 90% open area. They typically use a coarse support, often made of copper, gold or molybdenum. The reactivity of the coarse support can be an important issue in a static reactor, but will be of little consequence for the cross-flow approach. They are also available in much bigger sheets, for other possible experimental setups. The results here are calculated for standard TEM grids, and can be scaled for a much larger substrate. The substrates can easily pass 1 l/min of air at 1/10 to 1/100 of an atmosphere pressure drop without breakage, or without dislodging pre-absorbed particles. Nuclepore-type membrane filters have long been used to capture particles and sometimes to study reactions of them. However, they have too small a fraction of open area to provide the full advantage of a cross-flow.

Fig. (2) shows a simple mesh substrate, like lacey carbon or Quantifoil holey carbon membranes, being subjected to a cross-flow of gas. To limit wall effects in the tubing leading to the micromeshes, the flow rates should be kept high so that diffusion to the walls is limited during the transit time through them. One question is whether or not this flow is expected to be laminar or turbulent, either due to the shear of velocity on the scale of the tube delivering the gas to the mesh, or in the air flowing around the mesh structure itself. In a tube the flow is laminar, if the flow parameter, the Reynolds number, is less than 2300 [11]. This number is the average gas flow velocity times the tube inner diameter divided by the kinematic viscosity of air. Since these TEM micromeshes have a useful diameter of about 2.5 mm, we assume this is also the tube inner diameter, and a flow rate of 1 l/min is used. This gives a Reynolds number of about 531. Thus for flows up to about 4 l/min, the flow should be laminar in the tube delivering the gas to the substrate.

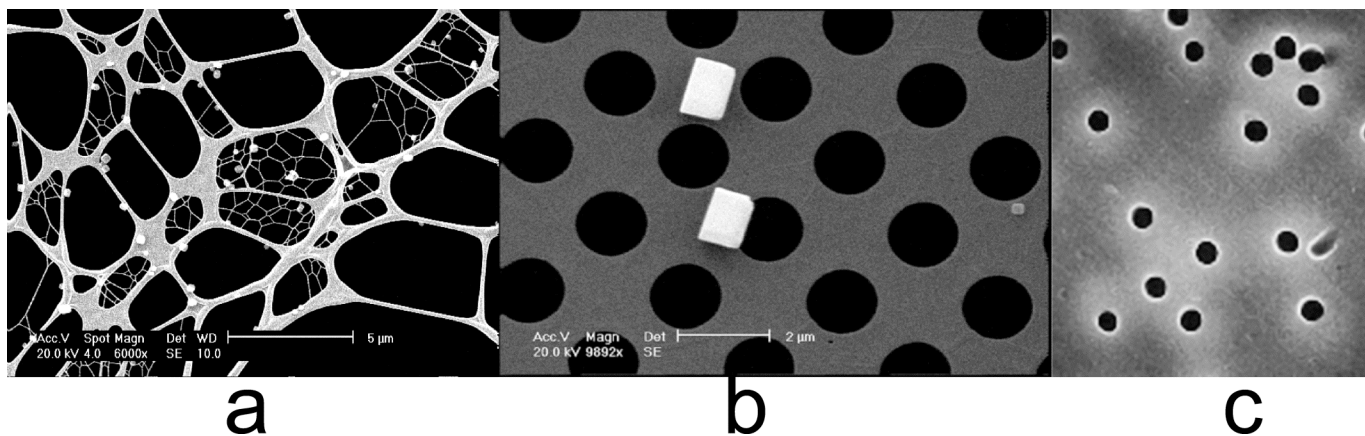


Fig. (1). (a) A scanning electron microscope image of 0.5 μm NaCl particles supported on a lacey carbon substrate (Electron Microscopy Sciences LC305-Cu). (b) A Quantifoil substrate (Quantifoil R1.2/1.3) with 1.5 micrometer NaCl particles. (c) A nuclepore membrane substrate (SPI-PoreTM membrane filter, 10-20,000 nm pore sizes).

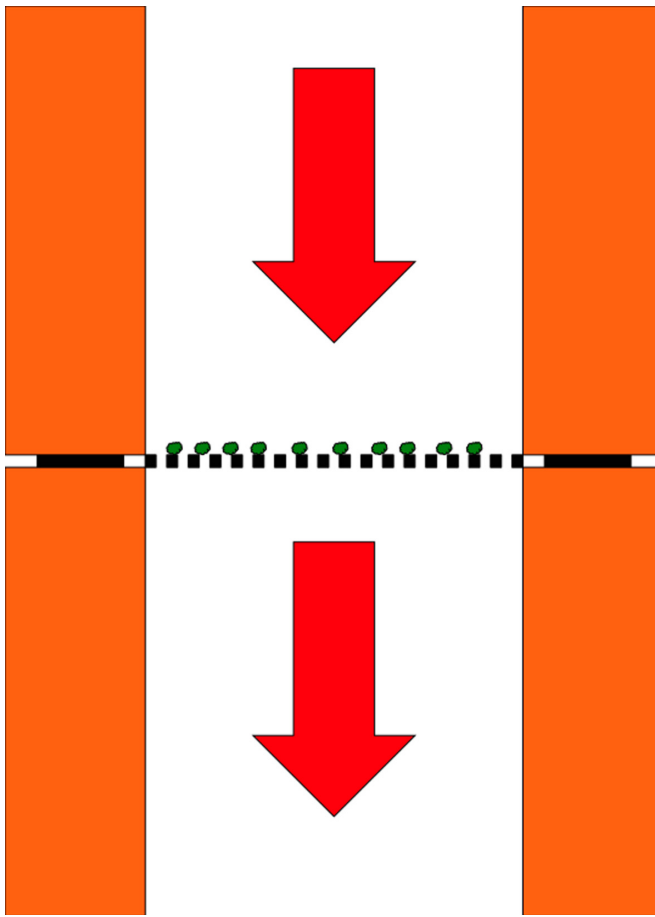


Fig. (2). A schematic diagram of the cross-flow through a substrate. Gas is brought to and away from the particles (green) that are supported on a micromesh (black) grid, *via* tubes (orange), and a pressure gradient across the micromesh.

The consideration for laminar flow near the micromesh grid element structure is more complicated, but still approximately the same, if the tube diameter is replaced with the mesh strand diameter. The local flow velocity is about twice that in the tube (for a 50% open mesh), and we assume the strand diameter is on the order of 1 micrometer. So the Reynolds number near the grid structure becomes (at 1 l/min) about 0.4. This is so low that the flow is guaranteed to be laminar around the micromesh grid elements.

In the following, we compare the transport issues for 1) an isolated single particle in a static gas, 2) multiple supported particles (M) in a static gas, and 3) M supported particles in the cross-flow configuration (see Fig. 2). We could do accurate numerical simulations for the effects of transport on each of these cases. But it is more important that we understand the comparisons at a fundamental level and under a wide range of parameters. For this reason, we treat the cases with some approximations that allow us to obtain analytical expressions for transport limitations. This will certainly make some answers in error at times by 50% or more, but it will allow us to better see how the comparisons depend on the parameters.

The general conditions we use when applying this analytical approach are: 1) the reactors are near atmospheric pressure, 2) particle diameters range from 0.1 to 1 μm , 3) tubing sizes and reactor diameters are on the order of

millimeters, and 4) the total number of particles are on the order of hundreds. These constraints make the physical parameters have a realistic size-order, for which the assumptions in our model work particularly well. In some cases it would be possibly misleading to extend the derived formulas and comparisons far without rechecking the validity of the assumptions. Our general “hierarchical” assumptions are that 1) the particle numbers are large (>100); 2) the pressure is high enough, that the mean free path (λ) is smaller than the reactor tube and mesh spacing and strand diameters; 3) λ is smaller than the average particle spacing on the substrate, and 4) λ is smaller than the particle diameter. We also assume that the substrate area is much larger than the particle area. We, for simplicity, assume plug flow of the gas in the reactor tube as it approaches the mesh reactor. This is usually accurate, as the mesh impedance is much higher than that of the tube wall.

The analytical results derived here are meant to design experiments that essentially eliminate transport limitations. They are not meant to provide extremely accurate estimates of the transport limited-rates. Avoiding transport limitations is crucial for experiments to determine accurate kinetics of aerosol reactions that can be applied to atmospheric conditions, where transport efforts are nearly absent.

3. RESULTS AND DISCUSSION

3.1. An Isolated Single Particle in a Static Gas

Fig. (3a) shows the gas transport around an isolated particle of radius R_p in a static gas. A single spherical particle immersed in a static gas initially at the trace gas density ρ_0 creates a disturbance. If we assume that ρ_0 is small enough (always so in our experiments) that the particle can reach a steady state with negligible change in particle composition, then for radial distances $r \gg R_p$, the trace gas density will still asymptotically approach ρ_0 . The trace gas will move in the vacuum between gas molecules on average a “mean free path” distance of λ , before it collides with another gas molecule. For simplicity, we treat the motion of the trace gas for $R_p < r < R_p + \lambda$ as if there are no gas phase collisions, with a source gas at a local density of ρ_1 . We also then assume for distances $r > R_p + \lambda$, that collisions dominate, and that simple continuum gas diffusion equations apply. This is done in most standard treatments [3, 12]. We here ignore corrections describing the depletion the Boltzmann velocity distribution of particles with positive radial velocities, as seen at $r = R_p + \lambda$, for high surface reaction probabilities. This effect, at most as large as 50%, can be easily added if desired. Ignoring it simplifies the equations, and it does not change the conclusions. We then simply equate the steady state bulk diffusion flow of the trace gas at the boundary $R_p + \lambda$, equal to $4\pi D(\rho_0 - \rho_1)(R_p + \lambda)$, to the net molecular dynamics transport, $\gamma_{\text{reac}}(4\pi R_p^2)\rho_1 \frac{c}{4}$, to solve for a consistent value for ρ_1 as in Eq. (1) [13],

$$\rho(r) = \rho_0 - (\rho_0 - \rho_1) \left(\frac{R_p + \lambda}{r} \right) \text{ for } r \geq (R_p + \lambda), \Rightarrow \rho_1 = \frac{\rho_0}{1 + \frac{R_p}{2\lambda} \left(\frac{\gamma_{\text{reac}}}{1 + \lambda/R_p} \right)} \quad (1)$$

This indicates that the trace gas density ρ_1 is a function of particle radius, particle reactivity, and diffusion mean free path. We use D (the gas diffusion constant $\approx 0.179 \text{ cm}^2\text{s}^{-1}$ for air at 1 atm) and use the common definition $D = \bar{c}\lambda/2$ here, essentially defining “collisions” as controlling diffusion. This gives λ (based upon D) as $\sim 0.067 \cdot 10^{-4} \text{ cm}$ at 1 atm [3] with \bar{c} the mean gas kinetic speed. To avoid transport limitations for a single particle, ρ_1 must be very close to ρ_0 . This requires $\gamma_p R_p / 2\lambda < 1$. For $\gamma_p \approx 1$ and the particle diameter of $1 \mu\text{m}$, we would need to reduce the total pressure (P) to less than 0.06 bar, in order to make $\lambda > R_p/2$, while for a $0.1 \mu\text{m}$ particle, the P can be as high as 0.6 bar. This well-known and very local transport problem is not the subject of this paper; rather the focus is the collective effects of many particles or the substrate reactivity.

3.2. Multiple Particles on a Substrate in a Static Gas

The case for M particles of radius R_p supported on a reactive disc substrate of radius $R_s \gg R_p$ placed on a non-reactive infinite plane reacting in a static gas does not yield a simple analytical expression. But a semi-quantitative analytical solution is easy and adequate to assess the limitations of this method. As a surrogate for M particles on a disc of radius R_s in a half space, we use $4 \cdot M$ particles on a spherical substrate of radius R_s in a full space as shown in Fig. (3b). The factor of 4 in particle numbers results from the difference in area between a circle and a sphere. This means that it has the same particle density as the original disk, on 4 times the area, in twice the space.

The particle and substrate reactivities are assumed to be γ_p and γ_s . Fig. (3b) shows a wavy contour, λ away from both the particles and the substrate. Locally for distances within this contour we assume as before that we have collisionless

molecular-dynamics-type motion, and at this contour we switch abruptly to continuum diffusional flow, at a local density of ρ_1 . However, the value of ρ_1 will be different if adjacent to a particle, than adjacent to the substrate. It will be $\rho_{1,p}$ and $\rho_{1,s}$, respectively. We define F_s and F_p , as the fractional areas of substrate and particles, with $F_p = 4M4\pi R_p^2 / (4M4\pi R_p^2 + 4\pi R_s^2)$ and $F_s = 1 - F_p$. We are assuming F_s is very near one. When R_p is comparable to or larger than λ , (as usual for our systems, $\rho_{1,s}$ can be very different than $\rho_{1,p}$). We pick a second spherical contour (Fig. 3b) at $r = R_s + H$, with H being a distance a few times of the lateral particle spacing. Assuming that $\lambda < H$, we make a rough approximation, that on this spherical contour at $r = R_s + H$ we are now seeing an average collective effect of the particles and substrate, and that there is a universally constant trace gas density of ρ_2 . We still assume that simple continuum diffusion applies for $r > R_s + H$. Equating flows of the trace gas at $r = R_p + \lambda$ near the local collective effects of particles plus substrate to that at $r = R_s + H$ gives Eq. (2):

$$\gamma_p (F_p 4\pi R_p^2) \rho_{1,p} \frac{\bar{c}}{4} + \gamma_s (F_s 4\pi R_s^2) \rho_{1,s} \frac{\bar{c}}{4} = 4\pi D (\rho_0 - \rho_2) (R_s + H) \quad (2)$$

If we assume that the particles are spaced much further apart than their diameter (not always true), then we can assume that the density moving away from each particle will go to the long range limit asymptote of $\rho_{1,s}$ with the latter taking the role of ρ_0 as in Eq. (1). This implies Eq. (3) around each particle:

$$\gamma_p (4\pi R_p^2) \rho_{1,p} \frac{\bar{c}}{4} = 4\pi D (\rho_{1,s} - \rho_{1,p}) (R_p + \lambda) \quad (3)$$

Next for $R_p \ll H \ll R_s$, we can (even when $\gamma_s = 0$) equate:

$$\gamma_s (4\pi R_s^2) \rho_{1,s} \frac{\bar{c}}{4} = 4\pi D (\rho_2 - \rho_{1,s}) \frac{1}{H} (R_s + \lambda)^2 \quad (4)$$

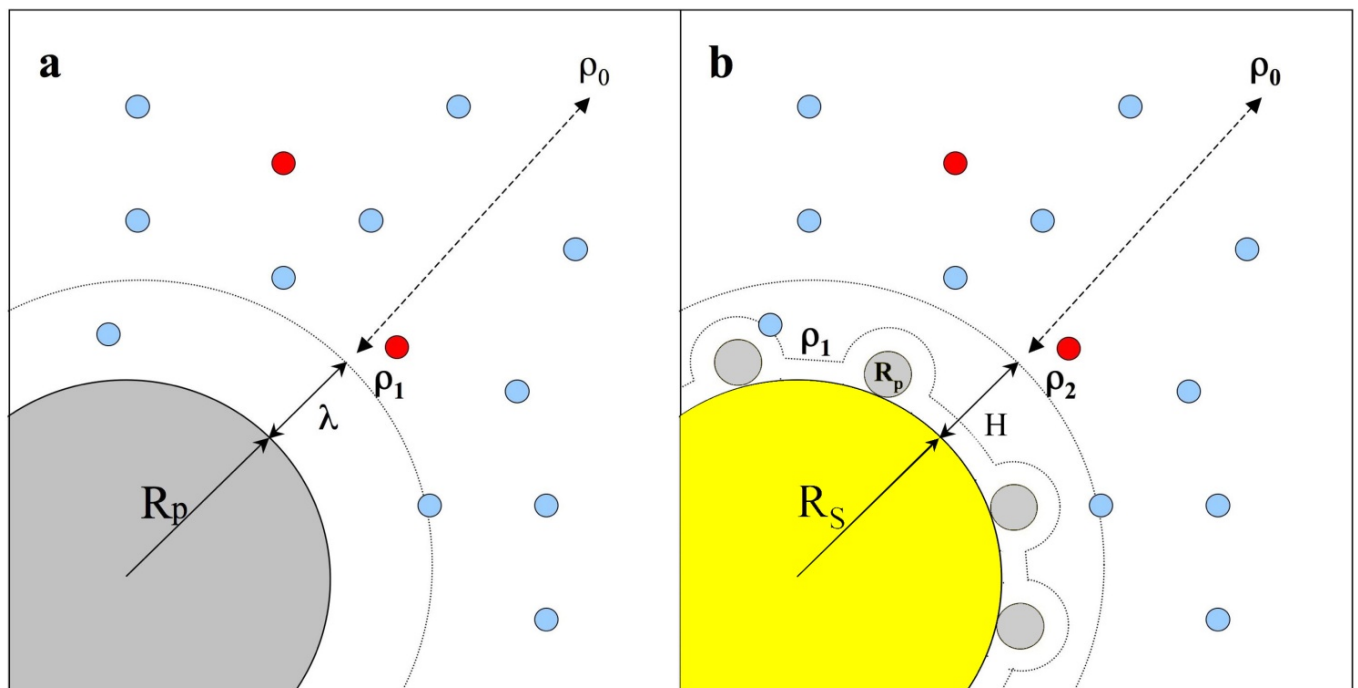


Fig. (3). (a) Gas transport around an isolated particle (grey) of radius R . Blue circles represent an inert background gas, and red circles represent reactive trace gas molecules. (b) Gas transport around $4M$ particles (grey) on a spherical substrate (yellow) of radius R_s .

Solution for $R_s \gg H \gg R_p$, $H \gg \lambda$, and $R_p \ll 2\lambda/\gamma_s$ gives Eq. (5),

$$\rho_{1,p} = \frac{\rho_0}{1 + \frac{R_p}{2\lambda} \left(\frac{\gamma_p}{1 + \lambda/R_p} \right) + \frac{R_s}{2\lambda} (F_p \gamma_p + F_s \gamma_s)} \quad (5)$$

Equation (6) shows Eq. (5) evaluated for a substrate diameter of 0.3 cm = 2R_s (used in [10] at 1 bar, and 2R_p=0.3 μm.

$$\rho_{1,p} = \frac{\rho_0}{1 + (0.77)\gamma_p + (9330)(F_p \gamma_p + F_s \gamma_s)} \quad (6)$$

While γ_p is usually the parameter that an experiment is trying to determine at ρ_0 , if we measure the extent of particle reaction, it will be that due to the local density $\rho_{1,p}$ from Eq. (6). We define the apparent reactive uptake coefficient γ_{app} as the ratio of $\rho_{1,p}/\rho_0$. Fig. (4) plots this γ_{app} versus particle number (top axis) and particle density (bottom axis) for particle reactivity $\gamma_p=0.5, 0.25$, and 0.005 , respectively, for the particular case of $2R_p=0.3 \mu\text{m}$. Since the particle is larger than the mean free path of the gas in this static system, some trace gas depletion near each particle occurs for $1 > \gamma_p \geq 0.1$. This can reduce the apparent reactivity (γ_{app}) ranging from substantially to slightly. However, the substrate effects can be much worse. For $F_s \approx 1$, a value of γ_s less than 10^{-5} is needed to determine γ_p , as shown in Fig. (5). Even if most of the substrate has $\gamma_s < 10^{-5}$, a small area of high reactivity will deplete the trace gas concentration over the whole sample. When $\gamma_s=0$, having too many particles still is unfavorable, that is, $F_p * \gamma_p \ll 10^{-5}$ is needed to keep trace gas from getting depleted.

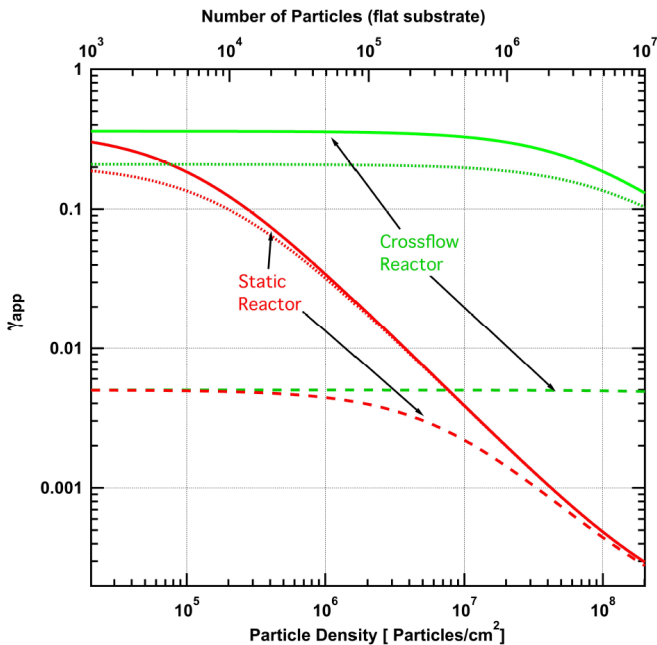


Fig. (4). The apparent reactive uptake coefficient γ_{app} versus number of particles (top axis) and particle density (bottom axis). The three red curves show the calculated particle density dependence of γ_{app} in a static reactor when γ_p equals to 0.5, 0.25 and 0.005 respectively from top to bottom. The three green curves show the calculated γ_{app} in cross-flow arrangement for γ_p of 0.5, 0.25 and 0.005 (top to bottom). We assume the substrate is non-reactive ($\gamma_s = 0$). The particle size is 0.3 μm in diameter. The substrate is 2.5 mm disc.

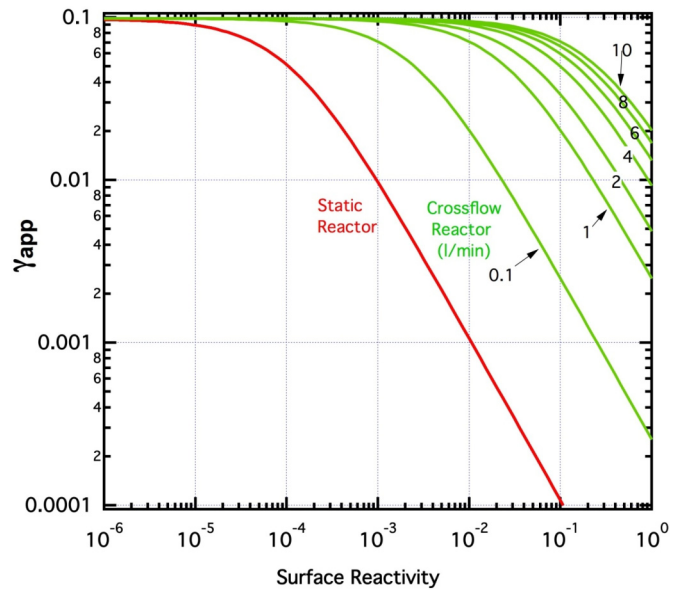


Fig. (5). The apparent reactive uptake coefficient γ_{app} versus surface reactivity, for $M=1000$ 1 μm diameter particles with $\gamma_p=0.1$. The red curve shows the results for the static reactor ($R_s=3$ mm), while the green curves the cross-flow reactor ($R_s=2.5$ mm) at flow velocities of 0.1, 1, 2, 4, 6, 8, and 10 l/min (bottom to top).

Even a modest number of particles in the static reactor severely deplete the trace gas as shown in Fig. (4). It requires $M < 1000$ on a 2.5 mm substrate to measure $\gamma_p=0.5$. This is feasible with single particle analysis techniques such as SEM or TEM, though it is very inconvenient. If we examine this plot to see if we can distinguish when $\gamma_p=0.25$ from $\gamma_p=0.5$, we see that for the static case this is only true for the lower particle part of the plot. Under most conditions shown, one cannot reliably distinguish a reaction probability of a factor of 2, for the static reactor case. Thus it is often not possible, even in principle, to take the transport-limited data, and obtain any meaningful value for γ_p .

3.3. Multiple Particles on a Substrate with a Cross-Flow

The advantage of using the cross-flow is that these transport effects can be greatly reduced. Let v_g be the velocity of the gas flow. In the disc arrangement v_g will depend somewhat upon the distance away from the filter. As shown below, if the gas flow is high enough, the significant transport limiting effects take place only very close to the filter surface. As discussed earlier, the flow is always laminar for our conditions. Our assumption of plug flow velocity near the micromesh is valid (except for where the gas (in a laminar fashion) swerves around the individual mesh strands and particles), because the impedance of the mesh is greater than that of the wall of the reactor tube. In Eq. (3), we treated the substrate as if it was a sphere (even though typically it is more likely a disc), to simplify the equations, which was a fair approximation as the transport effects are on the scale of the substrate diameter. For the flowing gas passing through the disc, the characteristic distances of collective transport limitations will shrink dramatically, to be less than the substrate diameter, even for very low flow rates. This will make the natural geometry to solve the equations to be planar.

The time (t) it takes for a trace gas molecule to be transported a distance Δz toward the substrate by the bulk gas flow is $\Delta z/|v_g|$. To travel this distance by diffusion alone takes about $(\Delta z)^2/D$. As Δz gets larger, the time for the transport to happen because of the gas flow always becomes shorter than the time for the trace gas to diffuse. Thus, over long distances the flow-induced motion of the trace gas is always faster than diffusion. For small enough Δz , diffusion is faster. The distance Z_1 , defined where the transport and diffusion times are equal, is given in Eq. (7):

$$t_{flow} \equiv \frac{Z_1}{|v_g|} = t_{diff} \equiv \frac{Z_1^2}{D} \Rightarrow Z_1 = \frac{D}{|v_g|} = \lambda \frac{\bar{c}}{2|v_g|} \quad (7)$$

Within the distance Z_1 of the reactive substrate (shown as the dashed box in Fig. 6), the trace gas flux is dominated by diffusion. Assuming the cross-flow reactor is of 2.5 mm diameter at 1 l/min flow, Z_1 is calculated to be 5.3 μm . This simplifies the situation significantly in two ways: First for z (the distance from the substrate) $> Z_1$, the gas density of the trace gas must approach ρ_0 regardless of the surface or particle reactivity. That this dimension is so short, \sim microns, means the distance scale of the transport limitations in the cross-flow configuration are greatly reduced, and as we shall see, so are the numerical effects of transport. Secondly, though the gas must flow around the particles and the grid substrate with a complicated vector flow field, it is not important to know that flow field. Typically for the particles of interest, R_p is less than 1 μm . and grid substrate strand diameters are less than 1 μm wide: these are smaller than Z_1 . Thus the diffusion velocities dominate trace gas flow near the particles and the grid strands. This means that we do not need to know the detailed vector flow field of the gas near the particles or the substrate grid, the faster short-range diffusion dominates. This diffusion really is not net diffusion (which requires a concentration gradient in Fick's law), but

instead the random walk diffusion that always occurs even with no concentration gradients, i.e. molecular Brownian motion. This does not require or imply that the trace gas density be constant for $z < Z_1$, just that the local gas flow velocity field becomes insignificant as the calculation shows.

Fig. (6) shows a model of the gas transport using the cross-flow over a substrate used in a configuration like that in Fig. (2). Now a planar geometry is the natural coordinate system. The same assumptions are used as in the static gas case close to the surface and particles (section 3.2, Fig. 3), with contours λ away from the surface and particles and $\rho_{1,s}$, $\rho_{1,p}$ being the local trace gas densities. The same lateral particle spacing H contour with ρ_2 is used as in Fig (3b). However, in this model we bridge the region between diffusive flow and hydrodynamic-flow-dominated trace gas transport by coupling these conditions to a locally Cartesian flow. As a result, Eq. (8) needs to be solved with z (distance from the substrate) and v_g (a gas flow velocity, negative in this case):

$$\frac{\partial \rho}{\partial t} = D \frac{\partial^2 \rho}{\partial z^2} - v_g \frac{\partial \rho}{\partial z} = 0 \Rightarrow \rho(z) = \rho_0 + (\rho_2 - \rho_0) e^{-\frac{(z-H)}{Z_1}} \quad \text{for } z > H, (Z_1 \equiv D/|v_g|) \quad (8)$$

$$\rho(z) = \rho_{1,s} \quad \text{for } -\infty \leq z \leq -H$$

Z_1 is the characteristic distance at which diffusion speeds match the bulk flow transport. For $z \ll -Z_1$ the trace gas density is just $\rho_{1,s}$, so the trace gas leaving the reactor is $\rho_{1,s} \times 4\pi R_s^2 \times v_g$. The amount entering the reactor from above is $\rho_0 \times 4\pi R_s^2 \times v_g$. The difference between the two is the gas consumed by the mesh plus particles. Equation (9) equates the two quantities using terms derived from Eq. (2):

$$\gamma_s (4\pi R_s^2) F_p \rho_{1,p} \frac{\bar{c}}{4} + \gamma_p (4\pi R_p^2) F_s \rho_{1,s} \frac{\bar{c}}{4} = |v_g| (4\pi R_s^2) (\rho_0 - \rho_{1,s}) \Rightarrow \gamma_s F_p \rho_{1,p} + \gamma_p F_s \rho_{1,s} = |v_g| \frac{4}{\bar{c}} (\rho_0 - \rho_{1,s}) \quad (9)$$

Using Eq. (9) and the same H and ρ_2 approach used in Eqs. (1)-(4), gives (for $R_p \gg \lambda$):

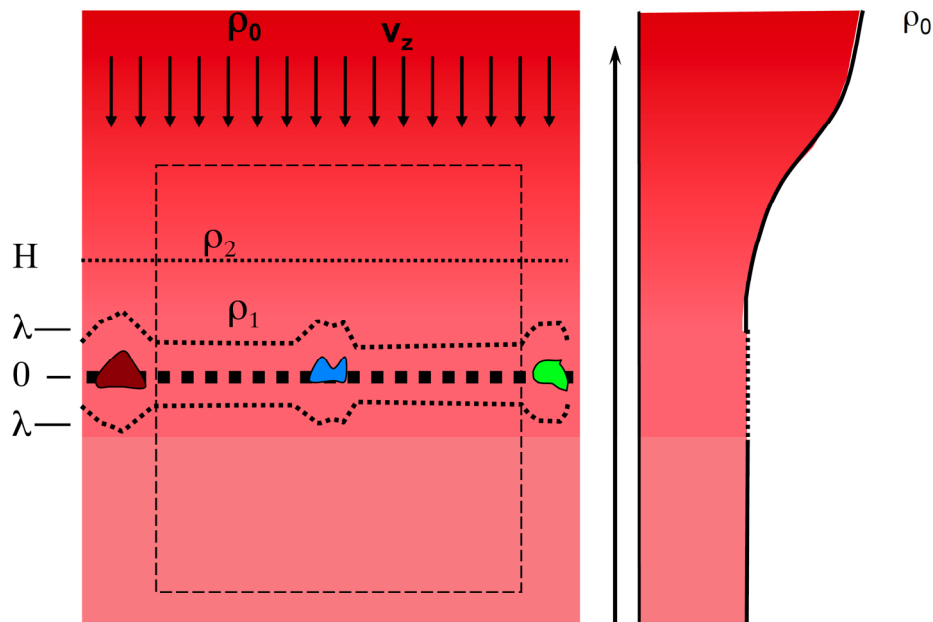


Fig. (6). A model showing gas transport in the cross-flow over a substrate. The z is the distance from the surface of substrate, and v_g is the gas linear flow speed (negative). The trace gas density is initially ρ_0 , and it is constant at ρ_1 for $z \leq \lambda$ (mean free path). The dashed square represents the “zone of isolation” that surrounds each particle (blue, brown, or green). Particles/substrate left, right, or below the zone cannot strongly interfere with reactions at its center.

$$\rho_{1,p} = \frac{\rho_0}{1 + \frac{R_p}{2\lambda} \left(\frac{\gamma_p}{1 + \lambda/R_p} \right) + \frac{Z_1}{2\lambda} (F_p \gamma_p + F_s \gamma_s)}, \text{ where } (Z_1 \equiv D/|v_g|) \quad (10)$$

Equation (10) also gives, $\gamma_{app} = (\rho_{1,p}/\rho_0) \gamma_p \cdot F_p$ is $M4R_p^2/(4MR_p^2 + R_s^2)$ (with M being the number of particles). Equation (10) is the fundamental result of this flow reactor case analysis. Now we evaluate Eq. (10) for a particular case, where a gas cross flow velocity $v_g = 1$ l/min and mesh region of the microgrid substrate of 2.5 mm diameter are used. This gives $v_g = -340$ cm/s ($\approx -0.01 \bar{c}$), and Eq. (11) is obtained for this specific case

$$\rho_{1,p} = \frac{\rho_0}{1 + (0.77)\gamma_p + (39)(F_p \gamma_p + F_s \gamma_s)} \quad (11)$$

3.4. Comparisons Between Cross-Flow and Static Conditions

Comparisons between static (Eq. (6)) and cross-flow conditions (Eq. (11)) show that for the conditions assessable in the cross-flow arrangement (using $v_g = 1$ l/min for calculations), the trace gas diffusion depletion caused by the substrate or collectively by the particles is from around 100 to over 1000 times less important than in the similarly sized static system. This is illustrated in Figs. (4, 5).

The cross-flow condition results remain accurate ($\gamma_{app} \approx \gamma_p$) for $\gamma_p = 0.005$ to over 10^8 particles/cm². For $\gamma_p = 0.5$, γ_{app} is decreased to $\gamma_p/(1+(0.77)*0.5)$ (the transport limit around each particle), but it is otherwise constant up to 10^7 particles/cm².

The cross-flow has another very important advantage over the static system: a natural, local, 3D “zone of isolation” extending Z_1 roughly spherically away from every point on the substrate, shown as a dashed square in Fig. (6). Interferences outside this zone do not affect the chemistry within it (except directly upstream). The fact that the zone of isolation extends laterally means that reactions occurring at any single (x, y) point on the substrate cannot be influenced by reactions taking place at any (or all) of the (x', y') points at a distance more than Z_1 away.

Perturbations of the reactive trace gases generated at (x', y') will be swept away by the flow field v_g , before it can diffuse over to exert influence at (x, y). Contaminations such as those from reactive metal holders further away than Z_1 are not a problem locally. This is very different and much better than using the static gas reactor, because in the latter case Z_1 is larger than R_s . Cross-flow also allows a good check for substrate reactivity. If the substrate was locally very reactive ($\gamma_s = 1$, for example), and locally depleting the trace gas, particles adsorbed within its zone of isolation will show less extent of reaction than those located further away. If the extent of particle reaction is observed to be constant over the substrate, then substrate reactions are either unimportant or at least very uniform!

Fig. (4) shows that if the number of particles (M) is large enough for them to collectively decrease the local trace gas density, γ_{app} will be considerably less than γ_p . The γ_{app} will then vary as $1/M$. Our cross-flow model does not show such sharp decrease in γ_{app} with M . For $|v_g| \approx 340$ cm/s, it is nearly not affected by particle overloading. A nice feature of the cross-

flow configuration is that the depletion of trace gas can be measured by looking at the composition of the exiting gas.

As per Eq. (4), the trace gas comes in at ρ_0 , and exits at $\rho_{1,s}$. Under many conditions $\rho_{1,s}$ is expected to be very close to ρ_0 . This can be measured in the cross-flow conditions. In contrast, a static reactor does not have this ability. One important question is whether or not the micromesh substrate is truly inert enough to avoid problems under the cross-flow, i.e. for $\gamma_s < 0.01$. The amorphous carbon used in SEM Quantifoil films and the lacey carbon is normally found to be remarkably inert (comparable to diamond or graphite). When the lacey carbon films are continuously exposed to gases like OH•, O₃, HNO₃, H₂O₂ in either the “stagnation cell” or in the static reactors [10, 14], substrate reactivity γ_s is typically less than 10^{-3} to 10^{-5} , arguably based on the observed magnitude of the apparent particle reactivities and the consistency of those measurements.

As shown in Fig. (5), even using a cross-flow at an air flow rate of 0.1 l/min dramatically improves the situation compared to the static system. For a very reactive substrate (or a very reactive reagent) flows as much as 10 l/min might be required. The results shown are for a 2.5 mm substrate.

It is a simple matter to use a substrate of larger areas, provided that the flow is scaled proportionally to the area. By using a much larger area, one could do long time aging of enough aerosols that subsequent wet chemical analysis would be easily possible. In a traditional coated flow tube, it is also possible to put large amounts of aerosols on the wall. But this easily (usually) creates severe transport limited reactions, which would then make it difficult to conduct meaningful kinetic studies. To avoid transport limited issues, the flowing air needs to flow right through the supported particles, not along them as in traditional flow tubes. We propose that porous wall reactors with transverse gas flow could in general be superior in supported particle reactive experiments. These would often permit wet chemical analysis of the eluted particles to measure reaction extents, with negligible transport limitations.

CONCLUSIONS

It is well-known that static reactors with supported particles have interferences from the substrate and collective particle reactivity in the form of “transport limitations” that easily grossly alter the results and make extraction of the true kinetics impossible. We have shown theoretically that pulling air through pre-deposited particles on microgrid substrates in cross-flow conditions is well-suited for long time atmospheric chemistry studies, because it is largely insensitive to transport limitations due to substrate reactivity or the collective effects of particles. It is around 3 orders of magnitude better in this regard than a similar sized stagnation approach using substrates of 2.5 mm diameter for conditions of 1 l/min velocity. The benefits can be scaled up in size without penalties, quite unlike the stagnation approaches. The cross-flow approach may make a very convenient replacement for very large aerosol chambers, the most commonly used technique for long time particle aging studies. The cross-flow naturally generates a micron-scale “zone of isolation” around each particle, inside of which diffusion dominates trace gas motion; while outside which the gas hydrodynamics dominates. This zone of isolation also strongly prevents the collective effects of other particles or substrate reactivity from causing trace gas depletion at each particle.

ACKNOWLEDGEMENTS

Support from a Department of Energy (DOE) Division of Chemical Sciences, Geosciences, and Biosciences grant (BES Chemical Sciences grant, KC-0301020-16248) and from a National Oceanic and Atmospheric Administration (NOAA) grant (GC05-358) is gratefully acknowledged. This work was performed at the Pacific Northwest National Laboratory operated for DOE by Battelle.

CONFLICT OF INTEREST

None declared.

ABBREVIATIONS

γ_{app}	= Apparent reactive uptake calculated from k_{meas} by assuming $\rho_1 = \rho_0$
γ_p	= Particle reactivity
γ_s	= Substrate reactivity or uptake coefficient of the substrate for the trace gas
λ	= Diffusion mean free path of a trace gas (≈ 0.067 micron at 1 atm)
ρ	= Density
ρ_0	= Background density of trace gas
ρ_1	= Trace gas density
$\rho_{1,p}$	= Density at a distance λ from the particles
$\rho_{1,s}$	= Density at a distance λ from the substrate
ρ_2	= Density at the distance of $R_s + H$
$\rho(r)$	= Trace gas density as a function of the radius
\bar{c}	= Mean gas kinetic speed
D	= Gas diffusion constant
F_s	= Fractional area of the substrate
F_p	= Fractional area of the particle
H	= A few times of the lateral particle spacing
k_{meas}	= Measured aerosol reaction rate
M	= Number of supported particles on a substrate of radius R_s
N	= Number of particles on a spherical substrate of radius R_s in a full space
R	= Radius
R_p	= Particle radius
R_s	= Radius of a reactive disc substrate
t	= Time
t_{flow}	= Time for gas flow transport
t_{diff}	= Time for diffusion
v_g	= Velocity of the gas flow

$ v_g $	= Magnitude of gas flow velocity
z	= Distance from the substrate
Δz	= Transport distance for a gas molecule
Z_1	= Distance where transport and diffusion are equal

REFERENCES

- [1] Intergovernmental Panel on Climate Change (IPCC). The physical science basis. In: Climate change 2007. Solomon S, Qin D, Manning M, *et al.*, Eds. Cambridge, United Kingdom: Cambridge University Press 2007; p. 996.
- [2] Pope CA III, Burnett RT, Thun MJ, *et al.* Lung cancer, cardiopulmonary mortality, and long-term exposure to fine particulate air pollution. *J Am Med Assoc* 2002; 287(9): 1132-41.
- [3] Seinfeld JH, Pandis SN. Atmospheric chemistry and physics: From air pollution to climate change. 1st ed. New York: John Wiley & Sons, Inc. 1997; p. 57.
- [4] Becker KH. Overview on the development of chambers for the study of atmospheric chemical processes, in Environmental simulation chambers: application to atmospheric chemical processes. Barnes I, Rudzinski K, Ed. NATO sciences series IV: earth and environmental sciences. Dordrecht, The Netherlands: Springer 2006; vol. 62: pp. 1-26.
- [5] Leu MT, Timonen RS, Keyser LF, Yung YL. Heterogeneous reactions of $\text{HNO}_3(\text{g}) + \text{NaCl}(\text{s}) \rightarrow \text{HCl}(\text{g}) + \text{NaNO}_3(\text{s})$ and $\text{N}_2\text{O}_5(\text{g}) + \text{NaCl}(\text{s}) \rightarrow \text{ClNO}_2(\text{g}) + \text{NaNO}_3(\text{s})$. *J Phys Chem* 1995; 99: 13203-12.
- [6] De Haan DO, Finlayson-Pitts BJ. Knudsen cell studies of the reaction of gaseous nitric acid with synthetic sea salt at 298 K. *J Phys Chem A* 1997; 101: 9993-9.
- [7] Underwood G, Li P, Usher CR, Grassian VH. Determining accurate kinetic parameters of potentially important heterogeneous atmospheric reactions on solid particle surfaces with a Knudsen cell reactor. *J Phys Chem A* 2000; 104: 819-29.
- [8] Hoffman RC, Kaleuati MA, Finlayson-Pitts BJ. Knudsen cell studies of the reaction of gaseous HNO_3 with NaCl using less than a single layer of particles at 298 K: A modified mechanism. *J Phys Chem A* 2003; 107: 7818-26.
- [9] Johnson ER, Sciegienka J, Carlos-Cuellar S, Grassian VH. Heterogeneous uptake of gaseous nitric acid on dolomite ($\text{CaMg}(\text{CO}_3)_2$) and calcite (CaCO_3) particles: A Knudsen cell study using multiple, single, and fractional particle layers. *J Phys Chem A* 2005; 109: 6901-11.
- [10] Laskin A, Wang H, Robertson WH, *et al.* A new approach to determining gas-particle reaction probabilities and application to the heterogeneous reaction of deliquesced sodium chloride particles with gas-phase hydroxyl radicals. *J Phys Chem A* 2006; 110: 10619-27.
- [11] Holman JP. Heat transfer. 9th ed. New York: McGraw-Hill 2002; p. 207.
- [12] Pruppacher HR, Klett JD. Diffusional growth and evaporation of water drops and snow crystals. In: Rosen RD, Ed. Microphysics of clouds and precipitation. Atmospheric and oceanographic sciences library. 2nd ed. Dordrecht, The Netherlands: Kluwer Academic Publishers 1997; vol. 18: pp. 505-7.
- [13] Ivchenko IN, Loyalka SK, Tompson Jr. RV. The free-molecular regime. In: Moreau M, Ed. Analytical methods for problems of molecular transport. Fluid mechanics and its applications. Dordrecht, The Netherlands: Springer 2007; vol. 83: pp. 91-140.
- [14] Krueger BJ, Grassian VH, Iedema MJ, Cowin JP, Laskin A. Probing heterogeneous chemistry of individual atmospheric particles using scanning electron microscopy and energy-dispersive X-ray analysis. *Anal Chem* 2003; 75(19): 5170-9.